A51A-0053

Ship observations of southeastern tropical Pacific stratocumulus clouds along 20°S

Simon P. de Szoeke[1], Chris W. Fairall[2], Casey D. Burleyson[3], Paquita Zuidema[4], and Sandra E. Yuter[3]

[1]Oregon State University, Corvallis, OR sdeszoek@coas.oregonstate.edu [2]NOAA Earth Systems Research Laboratory, Boulder, CO [3]North Carolina State University, Raleigh, NC [4]University of Miami, FL

Introduction

High-albedo marine stratocumulus clouds cool the top-of-atmosphere and surface radiation budgets over the eastern subtropical and tropical Oceans. Most models used for the IPCC 4th Assessment overpredicted net radiative warming by 10-30 W m^{-2} in the 20°S, 85-75°W region, partly explaining warm SST errors (de Szoeke et al. 2010). We measured clouds in the southeastern tropical Pacific along 20°S, describing their geometry and radiative forcing. Radar observations from EPIC and the VAMOS Ocean Cloud Atmosphere Land Study (VOCALS) Regional Experiment supplied unique observations that help determine to what degree drizzle controls clouds.

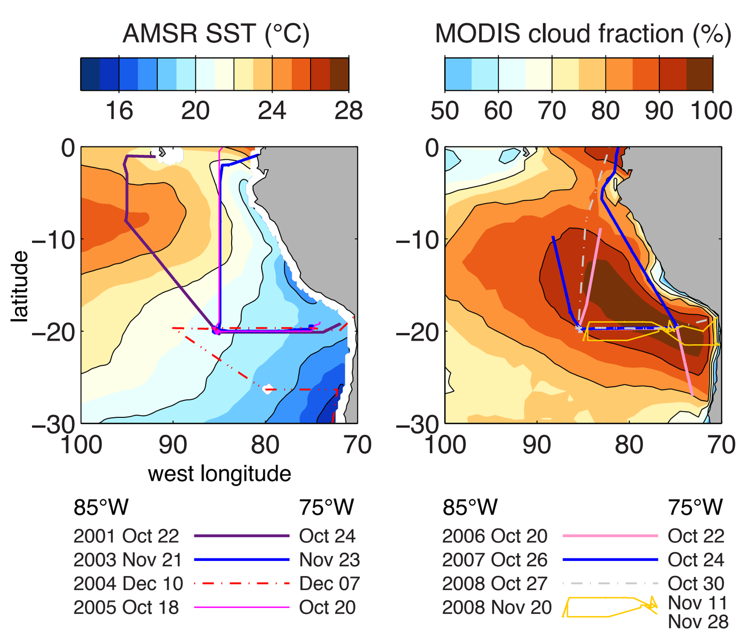

Figure 1. October-November satellite sea surface temperature (SST) and cloud fraction climatology in the southeastern tropical Pacific Ocean from the AMSR-E and MODIS instruments, respectively. Colored lines indicate tracks of NOAA research cruises included in the stratocumulus synthesis data set. Dates of reaching stations at 75° and 85°W are listed for each track in the key below.

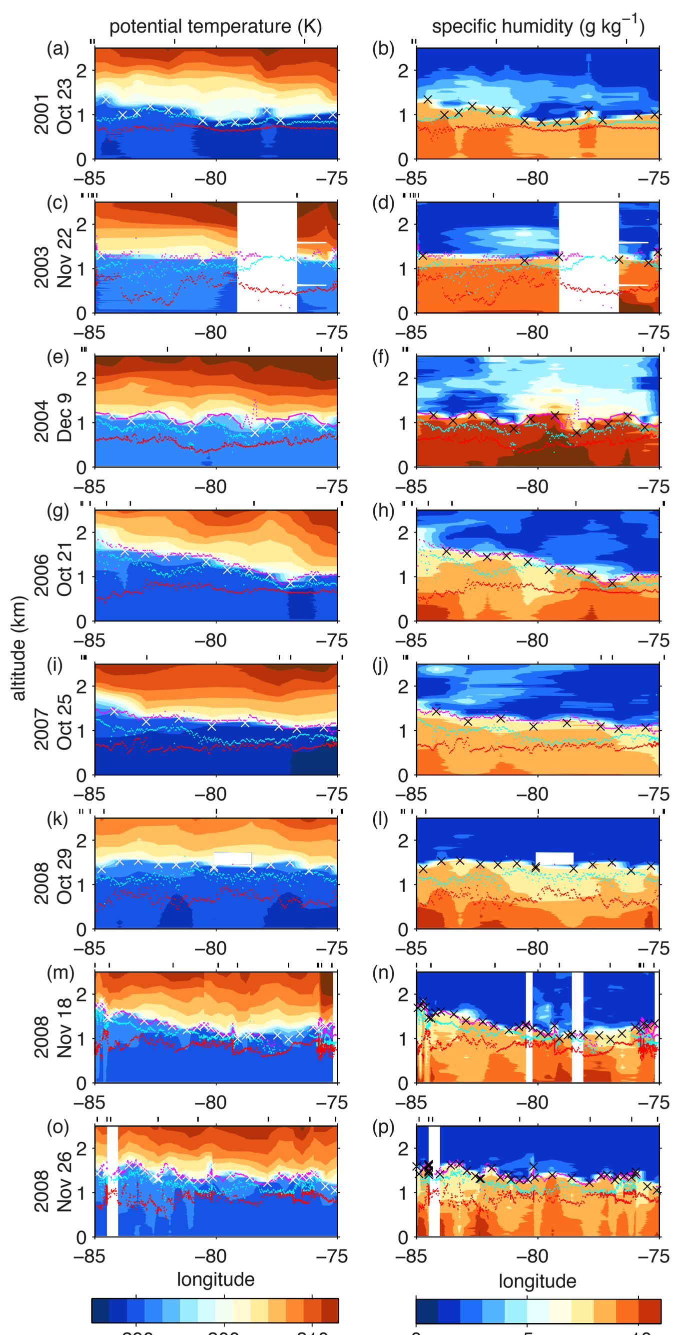

Figure 2. Eight sounding cross-sections of potential temperature and specific humidity along 20°S. Red points indicate lifting condensation level, blue points ceilometer cloud base height. Crosses show the inversion diagnosed from the temperature minimum for each sounding, magenta lines show the inversion diagnosed from remote sensing.

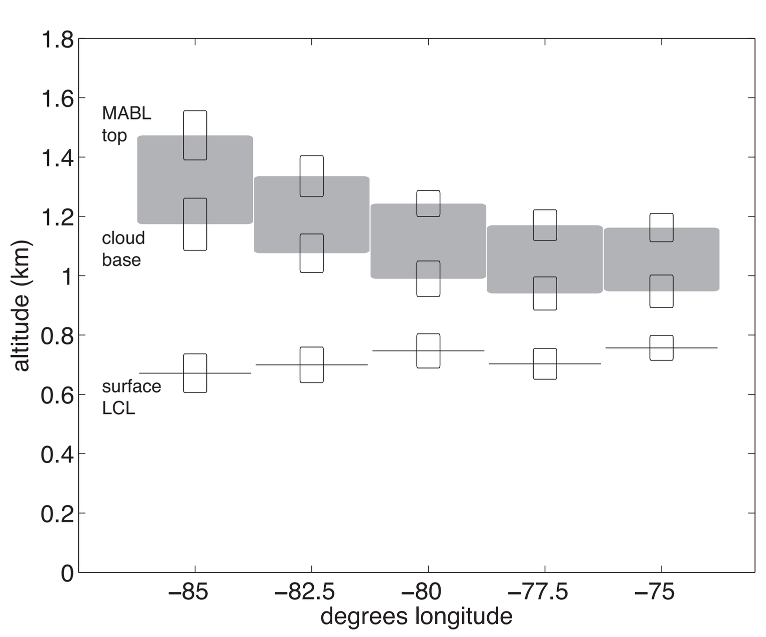

Figure 3. Mean cloud boundaries from ship remote sensing observations (gray boxes). Lifting condensation level (LCL) for a parcel with surface humidity and temperature (black lines). Unfilled boxes show mean plus and minus one standard error.

Soundings and cloud geometry

Multiple rawinsondes per day measured the well-mixed moist marine atmospheric boundary layer overlain by the dry stably-stratified free troposphere (Fig. 2). Figure 3 shows the cloud boundaries along 20°S, 75-85°W averaged in 2.5° longitude bins. Cloud thickness is constant, but there is a but cloud base and top rise westward. Lifting condensation level (LCL), diagnosed for measured surface meteorology, is relatively constant.

The displacement of cloud base height from LCL is a moist thermodynamic proxy for cloud decoupling that complements dynamical definitions of decoupling, e.g. inferred by comparing cloud base height to vertical velocity variance profiles (Tucker et al. 2009). The larger the cloud base–LCL displacement, the less mass is exchanged between the surface mixed layer and the cloud, and the greater the decoupling. Decoupling by this measure increases westward in Fig. 3.

Radiative fluxes

Figure 4 shows the mean downwelling (a) solar and (d) longwave radiation (filled circles) for 2.5-degree longitude bins, observed on the 7 years of research cruises. Shortwave radiation is daily averaged to avoid aliasing the diurnal cycle. Radiation changes less with longitude than sampling standard deviation in each longitude bin (boxes). Open circles show modeled clear-sky radiation.

Using overhead cloud fraction from the laser ceilometer, radiation is conditionally averaged for cloudy (Fig. 4b,e) and cloudy (Fig. 4c,f) skies. 67% of scenes have cloud fraction of 1, so cloudy averages are similar to those of full-sky. For clear skies radiative fluxes collapse to the clear-sky model. Figure 5 shows the solar transmissivity ratio, color coded by clear (magenta), cloudy (blue), and partly cloudy (black) skies diagnosed from the ceilometer. Curves show hourly lowpass filtered diurnal composites. Clear skies have transmissivity near one. Cloudy skies had maximum transmissivity in the afternoon at 13 local, and a minimum after sunrise.

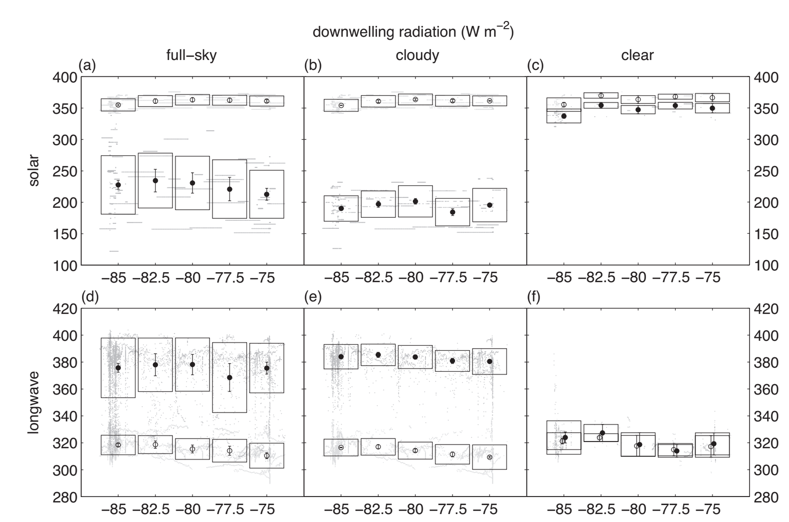

Figure 4. Solar and longwave surface downwelling radiation measured (filled circles) and simulated with a clear-sky model (open circles). Full-sky values (a,d); Cloudy conditions (b,e); clear conditions (c,f).

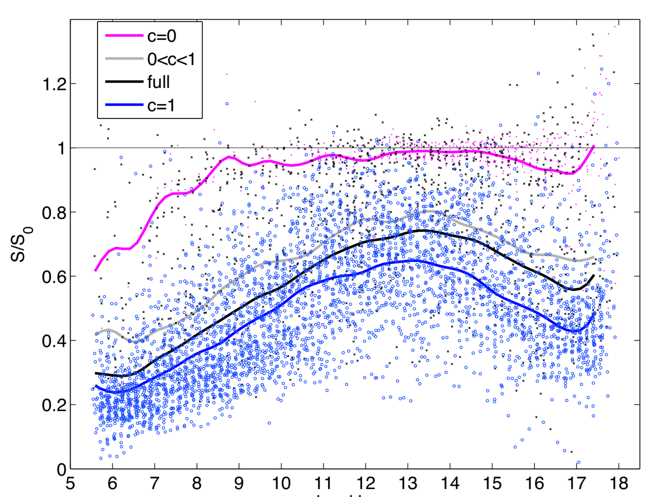

Figure 5. Daylight variation of solar transmissivity. Magenta dots are for ceilometer cloud fraction =0, blue dots are for cloud fraction=1. Black crosses are for 0<cloud fraction<1. Solid lines show the mean composited on the time of day.

Diurnal cloud decoupling

Cloud base–LCL displacement is composited on local hour in Fig. 6 (shaded). The mode of the displacement is small and constant at night, and rises steadily several after sunrise, to several 200-500 m in the evening (17 h). The aggregate distribution regardless of hour (curves at left) show both rising peak displacement and a broader distribution of displacement with longitude. Figure 7 shows scatter plots of cloud base height vs. LCL. Correlation between displacement is only strong in the afternoon, notably at 85°W (Fig. 7c).

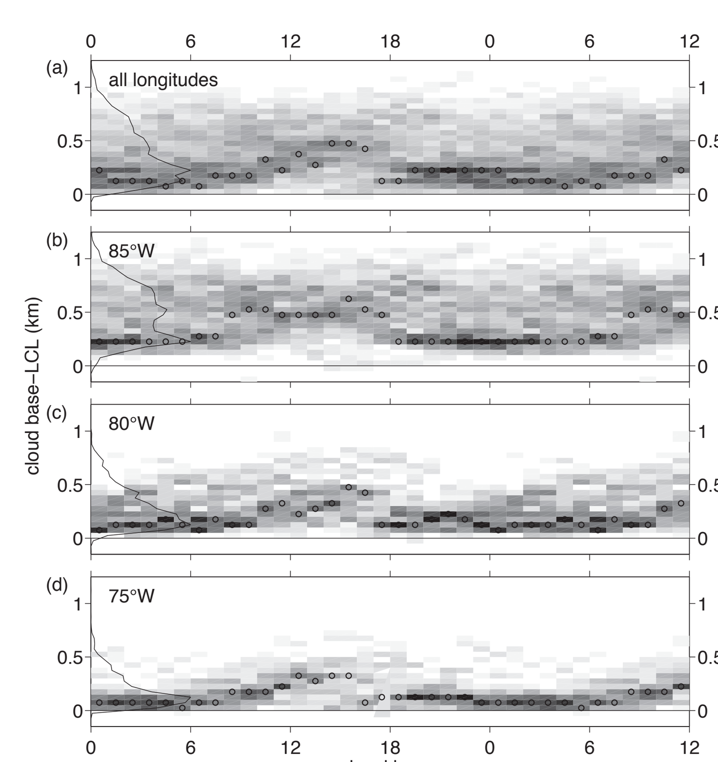

Figure 6. Diurnal cycle of vertical displacement of cloud base height from LCL for (a) all longitudes, (b) 85°W, (c) 80°W, and (d) 75°W, repeated for 1.5 day. Shaded squares show relative frequency in each panel, circles indicate the mode. Black lines on the left show normalized probability distributions for all hours.

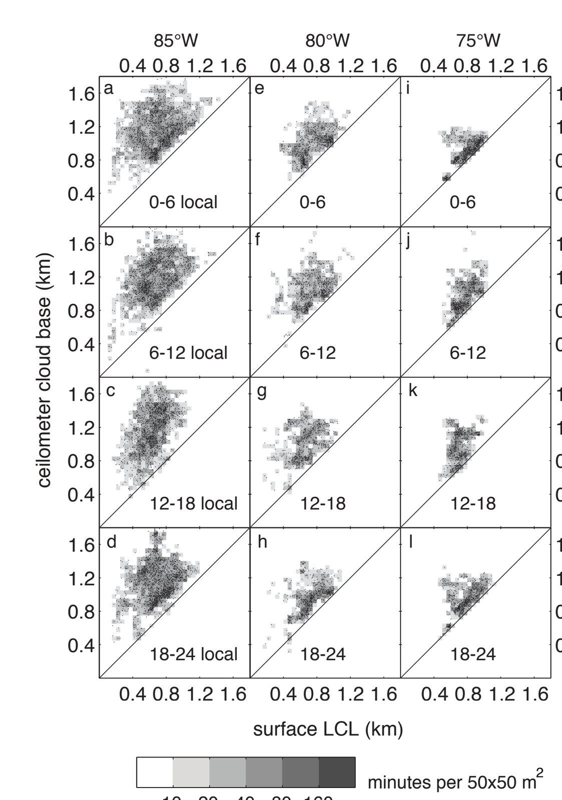

Figure 7. Diurnal cycle scatter plot of cloud base height vs. LCL in 4 intervals, 0-6, 6-12, 12-18, and 18-24 h local (rows); at three longitudes, 85°W, 80°W, and 75°W (columns). Black dots indicate coincident 10-minute LCL and cloud base height observations. Shaded squares show joint frequency of LCL and cloud base in 50x50 m^2 bins.

Cloud radar

Radar observations in 2008 from the NOAA 94 GHz cloud radar (Moran et al. 2010) remotely sense cloud and drizzle profiles. Figure 8 shows reflectivity and vertical velocity for 3.5 hours on 2008 Nov 20 intersecting a strongly drizzling cell. Joint histograms (Fig. 9) show the empirical relationships between Doppler velocity and reflectivity at different heights. The resolved velocity distribution width is ~1 m s^{-1}. At cloud top the mode of Doppler velocity is zero, while at and below cloud base downward velocities prevail. In weakly drizzling clouds (Fig. 11), the joint distribution resembles that at the top of the strongly drizzling cloud. Doppler velocity of rain on Nov 20 shows a quadratic dependence on dBZ.

The Doppler width is roughly half the velocity, implying a lognormal size distribution width of σ_x=0.25-0.5 (Frisch et al. 1995). Doppler velocity modeled from a lognormal size distribution with $N_{drizzle}$=1.5x10^3 m^{-2} and σ_x=0.35 is indicated by the red line.

November 20 11-14 UTC has strong drizzle.

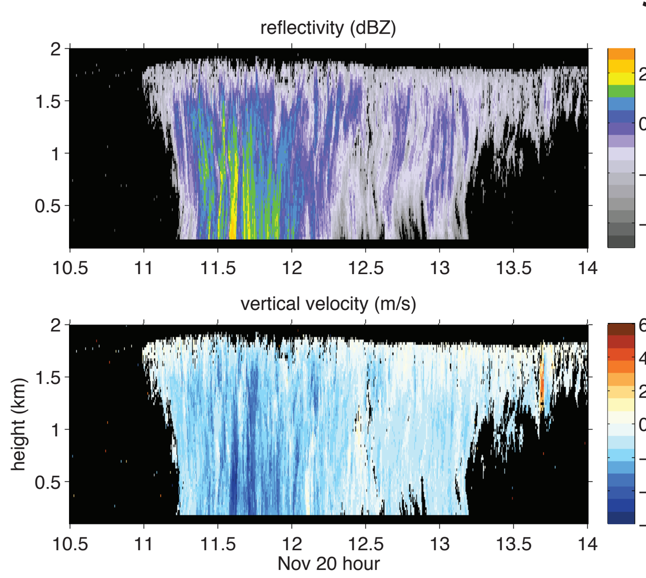

Figure 8. Reflectivity and Doppler velocity time-height section from cloud radar for 2008 Nov 20.

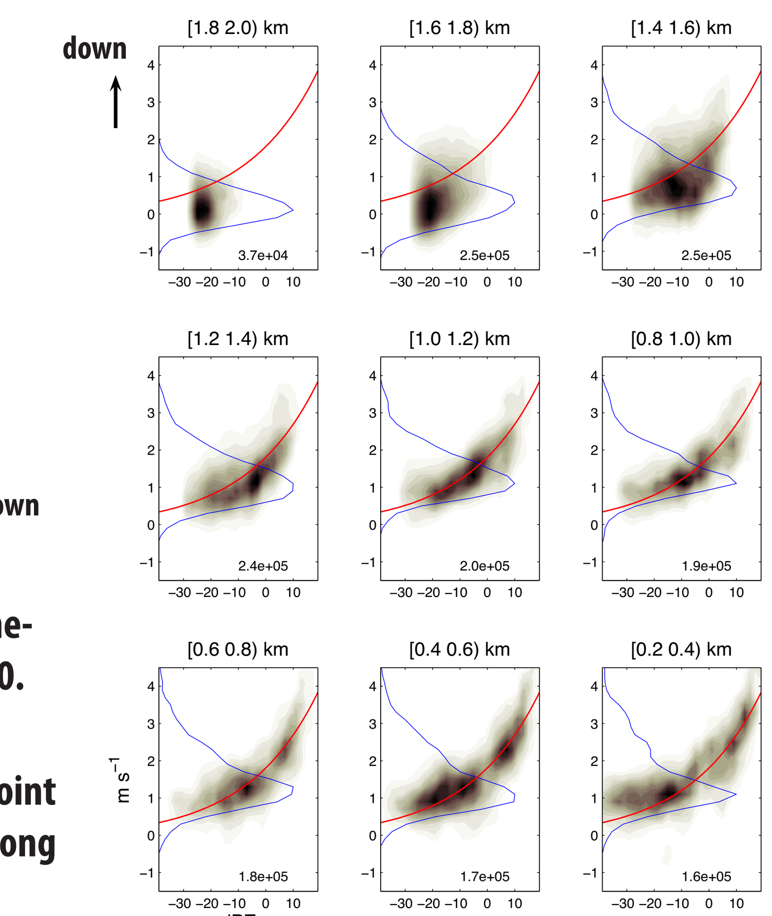

Figure 9. Reflectivity and Doppler velocity joint histograms for different height intervals in strong drizzle, Nov 20.

November 18, 4-8 UTC has little drizzle.

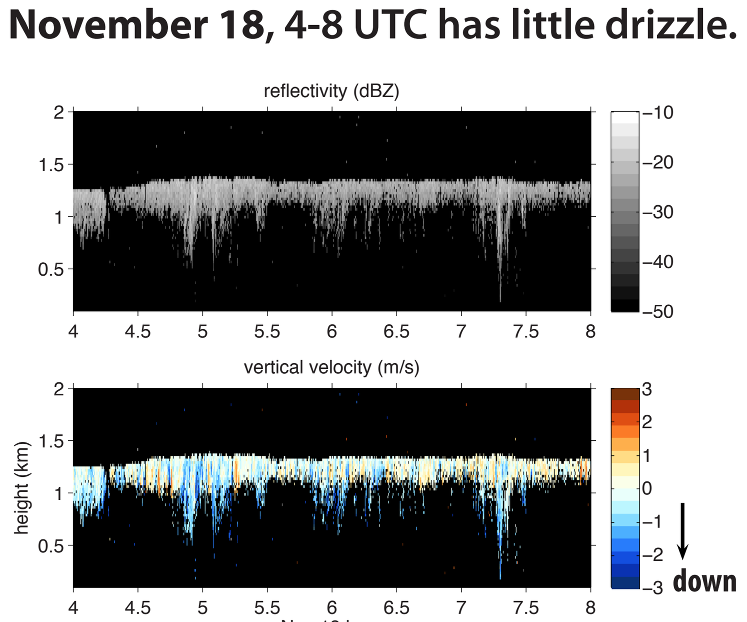

Figure 10. Reflectivity and Doppler velocity time-height section from cloud radar for 2008 Nov 18.

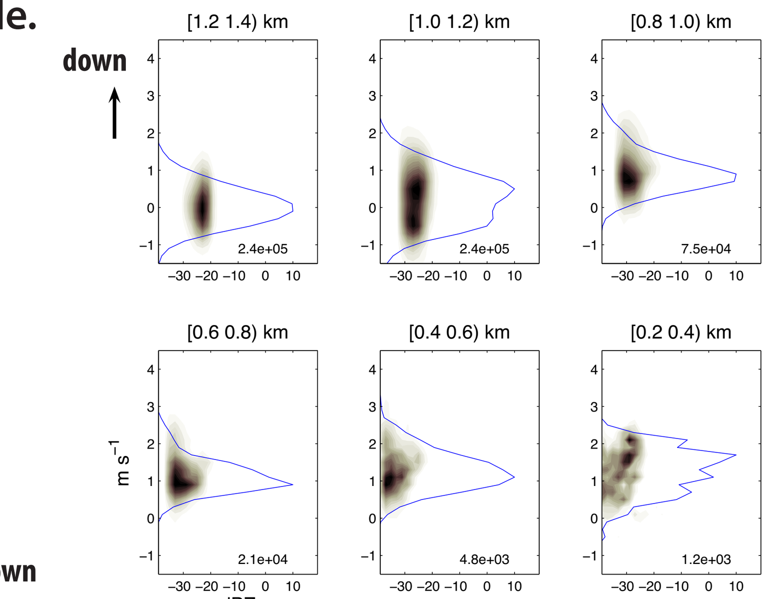

Figure 11. Reflectivity and Doppler velocity joint histograms for different 200-m height intervals with little drizzle, Nov 18. The number of observations is indicated in the lower right.

References

de Szoeke, Simon P., C. W. Fairall, D. E. Wolfe, L. Bariteau, P. Zuidema, 2010: Surface Flux Observations on the Southeastern Tropical Pacific Ocean and Attribution of SST Errors in Coupled Ocean–Atmosphere Models. *J. Climate*, **23**, 4152–4174.

Frisch, A. S., C. W. Fairall, and J. B. Snider, 1995: Measurement of Stratus Cloud and Drizzle Parameters in ASTEX with a Ka-Band Doppler Radar and a Microwave Radiometer. *J. Atmos. Sci.*, **52**, 2788-2799.

Moran, K., S. Pezoa, C. W. Fairall, T. Ayers, W. A. Brewer, C. Williams, S. P. de Szoeke 2010: A Motion Stabilized W-band Radar for Shipboard Observations of Marine Boundary Layer Clouds, *Boundary-Layer Meteorol.*, submitted.

Tucker, S., W. A. Brewer, S. Sandberg, A. Weickmann, D. E. Wolfe: Ship-based Doppler lidar studies of atmospheric decoupling under a Sc-topped MABL. 2nd VOCALS Science Meeting, July 2009.